Solid State Communications 147 (2008) 83–87

Contents lists available at ScienceDirect

Solid State Communications

journal homepage: www.elsevier.com/locate/ssc

Studies of nanostructures and conductivity in the system $V_xMo_{1-x}O_y$

Amreesh Chandra, Alexander J. Roberts, Robert C.T. Slade *

Department of Chemistry (C4), University of Surrey, Guildford GU2 7XH, United Kingdom

ARTICLE INFO

Article history:
Received 7 December 2007
Received in revised form
11 April 2008
Accepted 12 May 2008 by R. Phillips
Available online 15 May 2008

PACS:
81.07.Bc
82.45.FK
82.47.Uv
72.80.-r
82.45.Yz

Keywords:
A. Nanomaterials
A. Electrodes
B. Supercapacitor
D. Conductivity

ABSTRACT

Synthesis and characterization of the tailored nanostructured vanadium molybdenum oxide ($V_xMo_{1-x}O_y$) system is reported. TEM studies clearly show the formation of varying morphologies at vanadium and molybdenum rich ends. The effect of these differing morphologies on the surface area is presented. It is shown that compositions with $x < 0.40$ have electronic conductivity and a reduced contribution of ionic conductivity. Possible explanations for this observation are discussed. The VMO system shows promise for application as electrode materials in fields such as supercapacitors.

1. Introduction

Nano-materials and nano-composites, with the intrinsic advantage of large surface area and high aspect ratios, are being extensively investigated for application in energy storage systems such as Fuel cells, supercapacitors, batteries, etc. [1–6]. The power and energy storage capabilities of these devices are closely linked with the physical characteristics of the constituent electrodes [6–10]. Desired features of electrode materials include high conductivity, large surface area, low cost, controlled pore structure, thermal stability and reproducible synthesis [1,3,7,11]. In the case of supercapacitors, RuO_2 is the most commonly used metal oxide but the limiting factor is its cost [12,13]. Important metal oxides as alternatives to RuO_2 have recently attracted attention, and are based on vanadium oxide or related mixed oxide systems [14]. Most of the reported studies on mixed metal oxides have generally been done over a limited compositional range and the optimum synthesis route to obtain tailored materials remains a challenge.

We report the synthesis and characterization of the mixed vanadium molybdenum oxide, $V_xMo_{1-x}O_y$ (VMO), system across the complete compositional range, via a hydrothermal route [15] from V_2O_5 and MoO_3 starting materials. The exciting aspects of this study are enhanced surface area, raised electrical conductivity and the observation of nanorods/ nanoparticles, dependent upon composition. This study is a vital precursor to later implementation in supercapacitor technology.

2. Experimental

$V_xMo_{1-x}O_y$ nanotubes were synthesised via a hydrothermal route [15]. 1-hexadecylamine (0.025 mol) was added to deionised water (180 cm^3) and stirred for several hours. V_2O_5 and MoO_3 (total 0.025 mol) was added in the correct molar ratio and the suspension stirred vigorously for 7 days. The mixture was transferred to a Hastelloy stainless steel autoclave (Parr 4842) and heated to 140 °C with stirring for 24 h. The temperature was then raised to 180 °C for a further 48 h before cooling to room temperature. The resultant solids were collected by centrifugation, washed several times with deionised water and dried in air at 80 °C overnight. The dried materials were then heated to 450 °C in flowing nitrogen overnight to facilitate the removal of the 1-hexadecylamine template. Absence of 1-hexadecylamine was confirmed by thermogravimetry.

XRD powder profiles were recorded on a PANalytical X'Pert Pro PW PW3719 diffractometer using Cu K_α radiation and an X'Celerator detector. Samples for nitrogen sorption analysis were first outgassed at 200 °C for 12 h using a Micromeritics Flowprep 060 before transferring to a Micromeritics Gemini V Surface Area

* Corresponding author. Tel.: +44 1483 682588; fax: +44 1483 686851.
E-mail address: r.slade@surrey.ac.uk (R.C.T. Slade).

0038-1098/$ – see front matter © 2008 Elsevier Ltd. All rights reserved.
doi:10.1016/j.ssc.2008.05.012

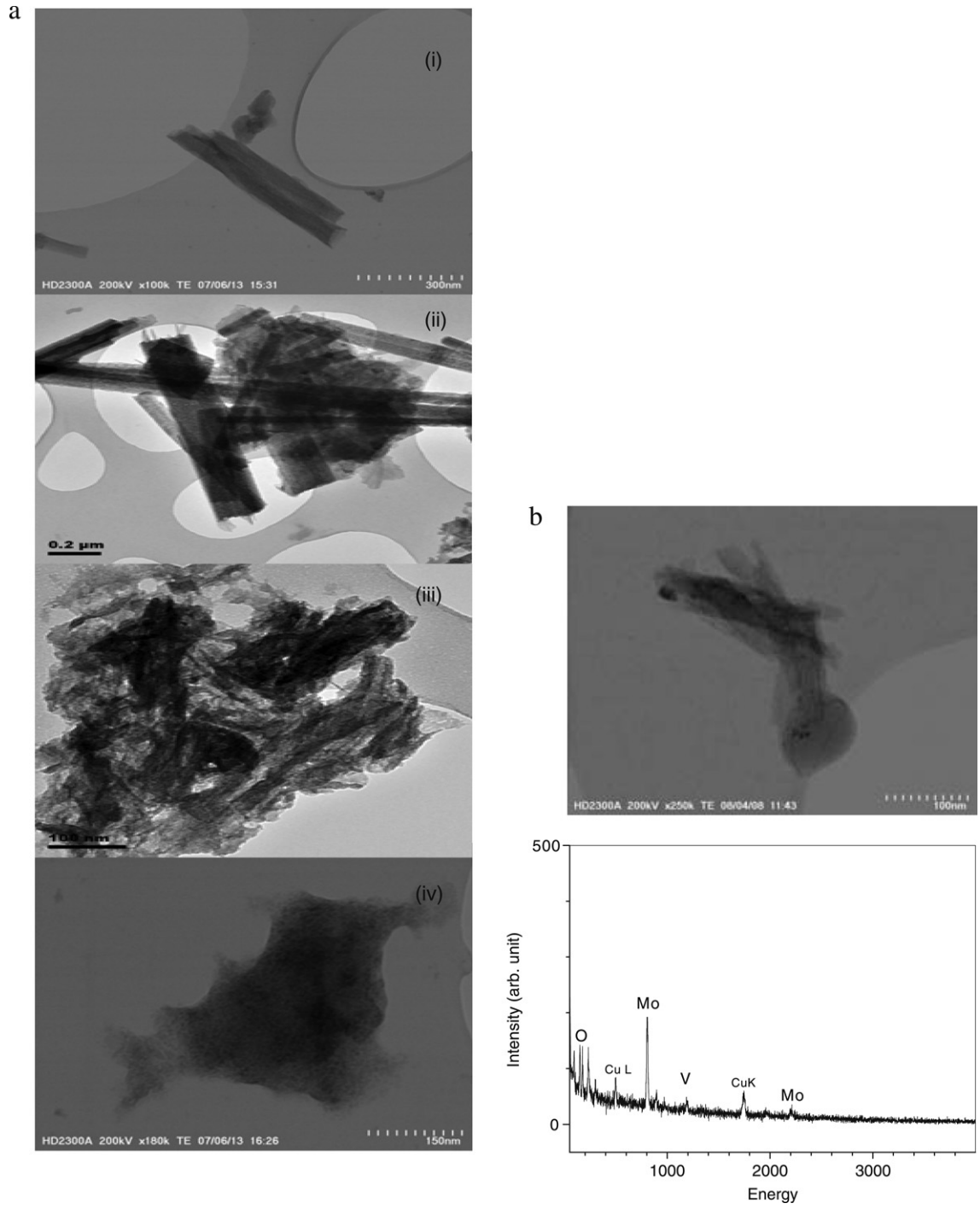

Fig. 1. (a) TEM micrographs of (i) VO_2, (ii) $V_{0.7}Mo_{0.3}O_y$, (iii) $V_{0.2}Mo_{0.8}O_y$ and (iv) MoO_3 (b) STEM micrograpahs and corresponding EDX curve obtained for $V_{0.2}Mo_{0.8}O_y$ sample. This clearly shows the coexistence of vanadium and molybdenum. The EDX signal showing presence of copper is from the copper grid on which the sample is deposited.

and Pore Size Analyser. Impedance measurements were carried out using a Solartron 1260 impedance analyzer in the frequency range 1 Hz–1 MHz (Oscillating voltage 0.5 V).

Typical TEM micrographs were recorded using a Philips/FEI CM200 instrument.

3. Results and discussions

Typical TEM micrographs of the VO_2, MoO_3 and intermediate compositions are shown in Fig. 1. A clear tubular morphology is observed at the nanoscale for the VO_2 sample (Fig. 1(i)), with tubes 400–600 nm in length and diameters 35–60 nm. It is suggested that VO_2 nanorods are formed by the coiling of V_2O_5 sheets around 1-hexadecylamine templates, with the subsequent removal of template and loss of oxygen during synthesis. Evidence of this can be seen upon close inspection of the coiled nature of the tubes. In the case of MoO_3 (Fig. 1(iv)) no tubular morphology is observed and the particles are seen to be agglomerations of smaller particles of the order of 3–10 nm in size. In the intermediate compositions, the coexistence of nanorods and nanoparticles are clearly observed (Fig. 1(ii,iii)). To clearly show that there is a coexistence of vanadium and molybdenum, STEM-EDX was also carried out.

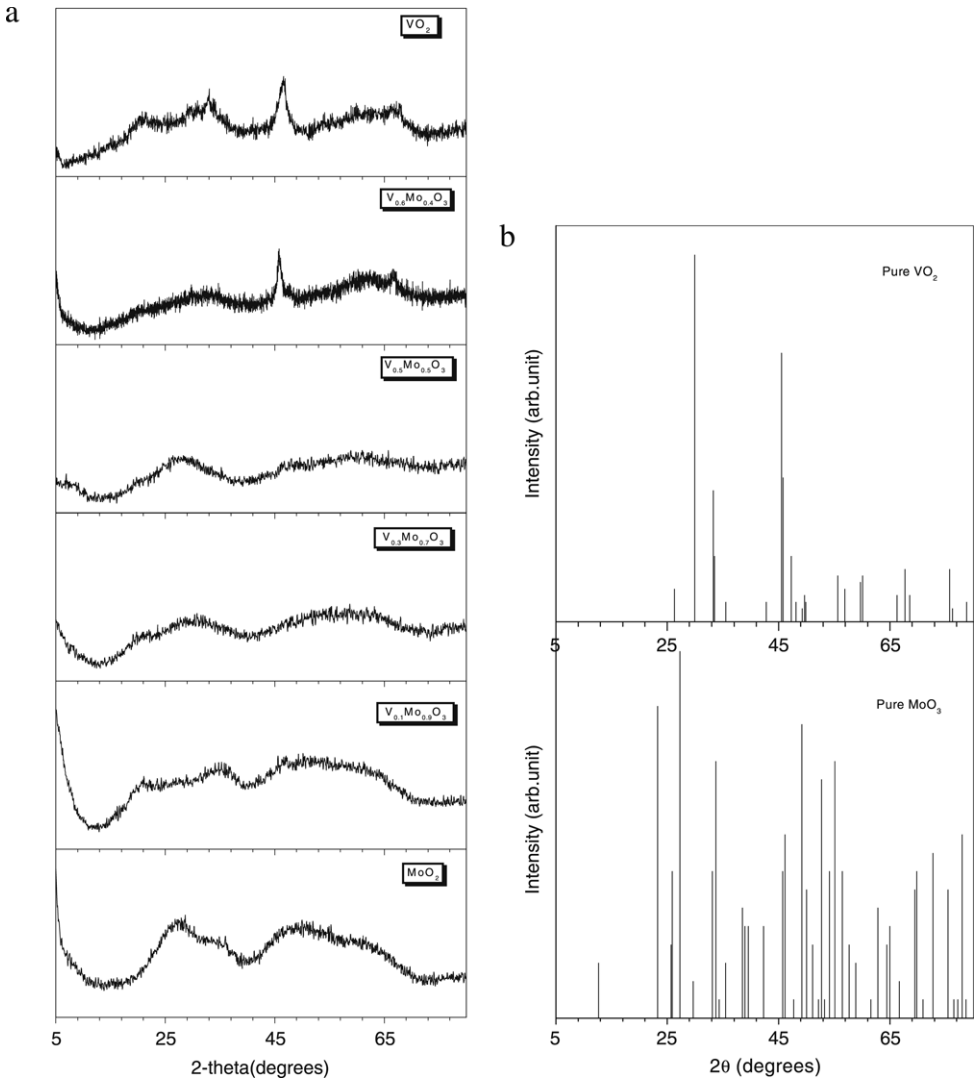

Fig. 2. (a) Evolution of X-ray diffraction pattern with x in the $V_xMo_{1-x}O_y$ system. (b) X-ray diffraction pattern of classical (i.e., pure) VO_2 and MoO_3.

Fig. 1(b)(i) shows the STEM micrograph for $V_{0.2}Mo_{0.8}O_y$ sample and the corresponding EDX data are shown in Fig. 1(b)(ii). This clearly confirms the coexistence of vanadium and molebdenum atoms in VMO samples; the EDX signal showing presence of copper is from the copper grid on which the sample is deposited. The significance of this widely differing morphologies and their coexistence will become evident below. The presence of distinct nanorods and nanoparticles suggests that the specific surface area and the conductivity of VMO will be composition dependent.

Fig. 2(a) shows the evolution of the XRD powder pattern of calcined $V_xMo_{1-x}O_y$ from one end composition ($x = 1$) to the other ($x = 0$). The major features are (i) absence of 'sharp peaks' corresponding to the unreacted starting components, (ii) systematic evolution of XRD patterns from pure VO_2 to pure MoO_3 (iii) broad Bragg scattering peaks clearly reconfirming the formation of nano-particulate systems observed in STEM and (iv) for $x < 0.40$ the system has predominantly broad Bragg reflections coming from the nanoparticles of MoO_3. For comparison, X-ray diffraction patterns of classical VO_2 and MoO_3 powders are given in Fig. 2(b).

Nitrogen sorption analysis at 77 K of all materials revealed isotherms displaying both type I and type IV behaviour as shown in Fig. 3. The adsorption branch of the isotherm showed a rapid uptake of nitrogen at low relative pressures but did not plateau, with hysteresis observed upon desorption consistent with the presence of both meso and micropores. The hysteresis loops could be classified as H3 combined with H4, suggesting of slit shaped pores formed through the aggregation of platy particles [16,17]. Specific surface areas calculated using the BET model were 56–148 m^2g^{-1}, with the highest being observed in the case of $x = 0.6$ and the lowest being MoO_3 ($x = 0$). Pore size distributions (BJH treatment) showed a modal pore diameter of 40 ± 3 Å. This was in agreement with values calculated from application of the Kelvin equation at the inception of the hysteresis loop (35.2–36.4 Å). Total pore volumes calculated from the plateau region of the hysteresis loop were 0.03–0.18 $cm^3\ g^{-1}$, the lowest being observed for MoO_3 ($x = 0$) and a local maximum at $x = 0.6$. As shown in Fig. 1, a nanotubular morphology is observed for vanadium oxides, with a considerably smaller dimensions being observed in the case of molybdenum oxides. The intermediate cases are a mixture of nanorods and nanoparticles. As expected, pore volumes calculated from N_2 sorption analysis are higher for the nanotubular materials than for Mo rich, with a local maximum being observed for $x = 0.6 - 0.7$. This local maximum is thought to be due to a favourable packing of the two morphologically distinct particles, maximising available pore space.

The real and imaginary parts of the electrochemical impedance spectra were also measured and the electrical conductivity evaluated. Typical plots of the composition dependence of electrical conductivity of VMO at two frequencies (viz. 610 kHz and

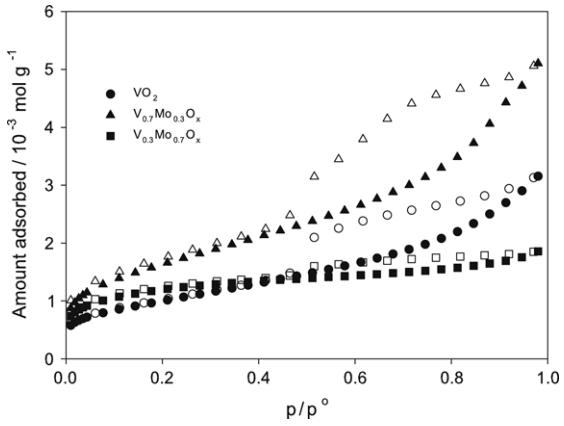

Fig. 3. Typical nitrogen sorption curve obtained at 77 K for VMO system. Closed symbols denote adsorption and open symbols denote desorption.

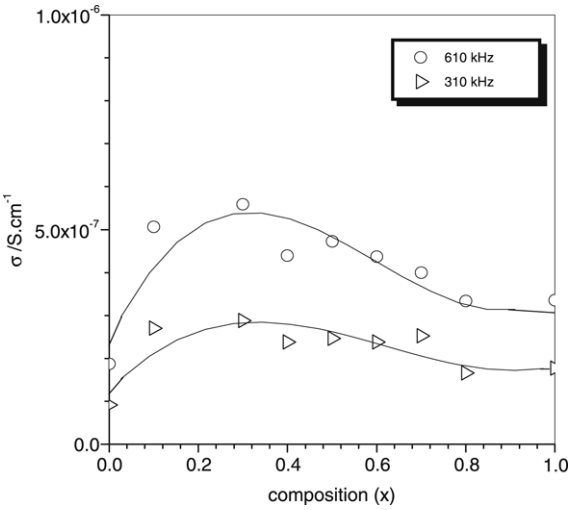

Fig. 4. Variation of conductivity with x in the $V_xMo_{1-x}O_y$ system. The solid line is drawn to act as guide to eye.

310 kHz) are shown in Figs. 4 and 5 shows complex impedance spectra for selected VMO samples. It is clear from Fig. 4 that the VMO samples in the mid composition range (i.e. $x \approx 0.3 - 0.7$) have relatively high conductivity in comparison to the end members, with the added advantage that the conductivity in this region is likely to be predominantly electronic and to become partially ionic towards the $x = 1$ limit. The partial ionic nature of conductivity can also be inferred from the impedance spectrum given in Fig. 5; the semi-circular plots obtained for V rich end of VMO system (Fig. 5(a) and (b)) are typical of those observed for ionic conductors. Vanadium based systems are known to take up water. Therefore, the ionic conduction may arise from H^+ and/or OH^- ions supplied by the increased number of water molecules and acid-base behaviour associated with the VO_2 nano-rods. It is also to be noted that for MoO_3-rich VMO samples ($x < 0.4$), the impedance spectra (Fig. 5(c) and (d)) show no semicircle and their nature is similar to that expected for electron/hole conduction in semi-conductors. The composition dependence of conductivities observed show a similar trend to the pore volume observed. At compositions of $x < 0.4$ the conductivity observed is predominantly electronic, with an increasing ionic component being observed as x increases. This is thought to be due to the

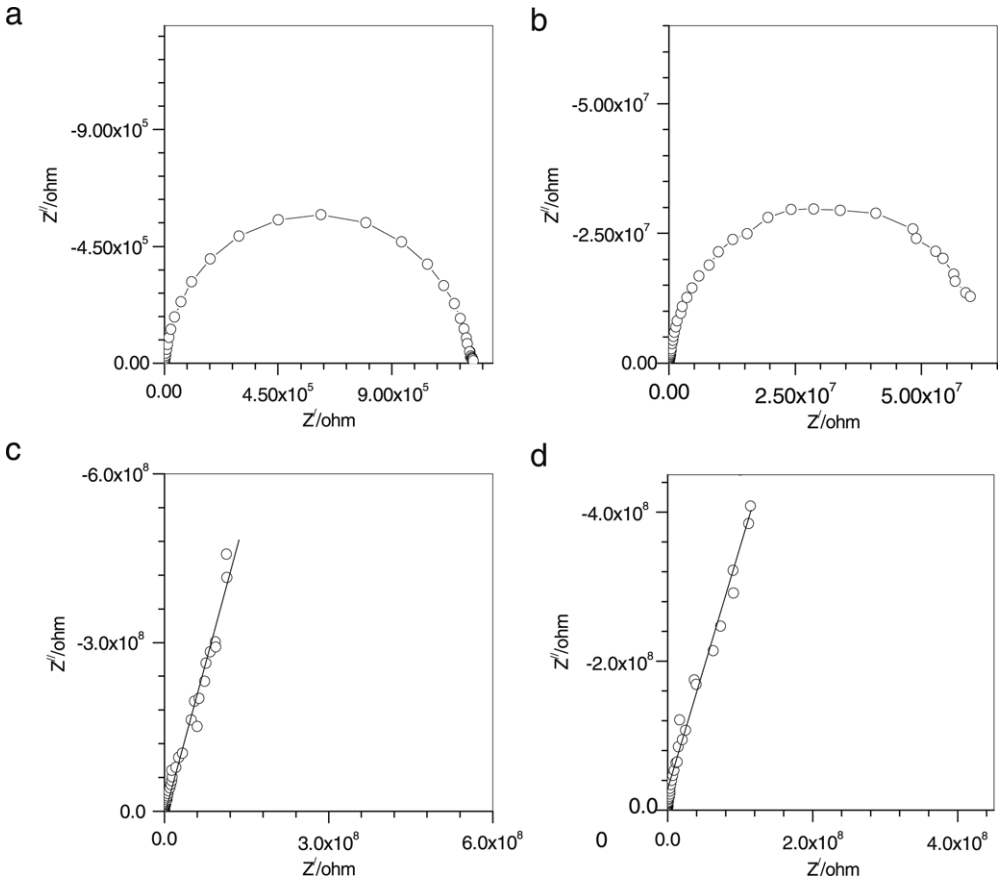

Fig. 5. Impedance spectra for four typical composition of $V_xMo_{1-x}O_y$ system: (a) $x = 1.0$, (b) $x = 0.70$, (c) $x = 0.30$ and (d) $x = 0.0$.

increase in available water as the pore volume and nanotubular fractions increase.

4. Conclusions

In conclusion, it has been shown that the nanostructured VMO system has a range of surface area and electrical conductivity that may be tailored through synthetic stoichiometry and methodology. The VMO compositions having $x = 0.6 - 0.3$ are promising materials for application as electrode materials, with the added advantage of being considerably cheaper than the commonly used RuO_2-based electrode materials for supercapacitors.

Acknowledgements

This work is funded under the EPSRC Supergen Energy Storage Consortium (Grant No. EP/D031672/1). We thank Miss B. Carroll and Dr. Y.L. Chen for assistance with electron micrography.

References

[1] V.L. Pushparaj, M.M. Shaijumon, A. Kumar, S. Murugesan, L. Ci, R. Vajtai, R.J. Linhardt, O. Nalamasu, P.M. Ajayan, Proc. Natl. Acad. Sci. 104 (2007) 13574.
[2] Q. Wang, Z. Wen, J. Li, Adv. Funct. Mater. 16 (2006) 2141.
[3] A.K. Cuentas-Gallegos, M. Lira-Cantu, N. Cason-Pastor, P. Gomez-Romero, Adv. Funct. Mater. 15 (2005) 1125.
[4] A.K. Cuentas-Gallegos, R. Maryinez-Rosales, M. NBaibarac, P. Gomez-Romero, M.E. Rincon, Electrochem. Comm. 9 (2007) 2088.
[5] G. Lota, K. Lota, E. Frackowiak, Electrochem. Comm. 9 (2007) 1828.
[6] Q.L. Chen, K.H. Xue, W. Shen, F.F. Tao, S.Y. Yin, W. Xu, Electrochim. Acta 49 (2004) 4157.
[7] J. Chmiola, Y. Yushin, Y. Gogotsi, C. Portet, P. Simon, P.L. Taberna, Science 313 (2006) 1760.
[8] A.K.C. Gallegos, M.E. Rincon, J. Pow. Sour. 162 (2006) 743.
[9] E. Frackowiak, V. Khomemko, K. Jurewicz, K. Lota, F. Beguin, J. Pow. Sour. 153 (2006) 413.
[10] C. Merino, P. Soto, E.V. Ortego, J.M.G.d. Salazar, F. Pico, J.M. Rojo, Carbon 43 (2005) 551.
[11] B.E. Conway, Electrochemical Supercapacitors, Kluwer Academia/Plenum Publishers, New York, 1999.
[12] W. Sugimoto, K. Yokoshima, Y. Murakami, Y. Takasu, Electrochim. Acta 52 (2006) 1742.
[13] Y.R. Ahn, M.Y. Song, S.M. Jo, C.R. park, D.Y. Kim, Nanotechnology 17 (2006) 2865.
[14] D. Sun, C.W. Kwon, G. Baure, E. Richman, J. MacLean, B. Dunn, S.H. Tolbert, Adv. Funct. Mater. 14 (2004) 1197.
[15] M. Niederberger, F. Krumeich, H.J. Muhr, M. Muller, R. Nesper, J. Mater. Chem. 11 (2001) 1941.
[16] F. Rouquerol, J. Rouquerol, K. Sing, Adsorption by Powders and Porous Solids, Academic Press, London, 1999.
[17] J. Rouquerol, D. Avnir, C.W. Fairbridge, D.H. Everett, J.H. Haynes, N. Pernicone, J.D.F. Ramsay, K.S.W. Sing, K.K. Unger, Pure Appl. Chem. 66 (1994) 1739.